Taylor & Francis
Taylor & Francis Group

Particulate Science and Technology

An International Journal

ISSN: 0272-6351 (Print) 1548-0046 (Online) Journal homepage: https://www.tandfonline.com/loi/upst20

Drag Force, Drag Torque, and Magnus Force Coefficients of Rotating Spherical Particle Moving in Fluid

N. Lukerchenko , Yu. Kvurt , I. Keita , Z. Chara & P. Vlasak

To cite this article: N. Lukerchenko , Yu. Kvurt , I. Keita , Z. Chara & P. Vlasak (2012) Drag Force, Drag Torque, and Magnus Force Coefficients of Rotating Spherical Particle Moving in Fluid, Particulate Science and Technology, 30:1, 55-67, DOI: 10.1080/02726351.2010.544377

To link to this article: https://doi.org/10.1080/02726351.2010.544377

Particulate Science and Technology, 30: 55–67, 2012

ISSN: 0272-6351 print/1548-0046 online
DOI: 10.1080/02726351.2010.544377

Taylor & Francis
Taylor & Francis Group

Drag Force, Drag Torque, and Magnus Force Coefficients of Rotating Spherical Particle Moving in Fluid

N. LUKERCHENKO,[1] YU. KVURT,[2] I. KEITA,[1]
Z. CHARA,[1] AND P. VLASAK[1]

[1]Institute of Hydrodynamics of the Academy of Sciences of the Czech Republic, v. v. i, Prague, Czech Republic
[2]Institute of Problems of Chemical Physics of the Russian Academy of Sciences, Chernogolovka, Moscow Region, Russia

The mutual influence of translational and rotational spherical particle movements in calm water was studied using experimental data and numerical simulation. Spherical balls with a density close to that of water were speeded up in special devices, which ensured the required ball rotational and translational velocity in the given plane. A video system was used to record the ball trajectory in water. The values of the drag force, Magnus force, and drag torque coefficients were determined experimentally and compared with the results of the numerical simulation of the particle motion. The evaluation of the experiments focused on the effects of two dimensionless parameters of the particle motion: the translational Reynolds number (or Reynolds number) and rotational Reynolds number. The experiments were carried out for the relatively slow (the dimensionless angular velocity $\Gamma < 3.5$) and relatively fast ($5 < \Gamma < 10$) particle rotation. Relationships describing the abovementioned coefficients were developed, taking into account the mutual influence of the translational and rotational particle movements. It was found that the drag force and drag torque coefficients can be expressed as the functions of both the translational and rotational Reynolds numbers.

Keywords drag force, drag torque, Magnus force, Reynolds number, rotational Reynolds number

Introduction

Models of spherical particles moving in fluid are often used for calculations of the conveyance of solid particles (Nino and Garcia 1994; Kholpanov and Ibyatov 2005; Chara et al. 2009; Lukerchenko et al. 2009a, 2009b). These models require

The authors would like to acknowledge the financial support provided by the Academy of Sciences of the Czech Republic under the Institutional Research Plan No. AV0Z20600510 and by the Grant Agency of the Academy of Sciences of the Czech Republic (Project No. IAA 200600603) and by the Grant Agency of the Czech Republic (Project No. GA 103/09/1718). The authors would also like to thank J. Miles for technical support for the experiments.

Address correspondence to P. Vlasak, Institute of Hydrodynamics of the Academy of Sciences of the Czech Republic, v. v. i. Pod Patankou 30/5,166 12, Prague 6, Czech Republic. E-mail: vlasak@ih.cas.cz

the correct definition of the forces and torques acting on the particle. The motion of a spherical particle in fluid near solid wall results to the particle-wall collisions and the sequent particle rotation. The sphere translational motion with simultaneous rotation in fluid is characterized by two dimensionless parameters: translational Reynolds number (or Reynolds number) $\mathrm{Re} = |\bar{V}|\,\mathrm{d}/\nu$ and rotational Reynolds number $\mathrm{Re}_\omega = |\bar{\omega}|\,\mathrm{r}^2/\nu$, where d is the sphere diameter, $\mathrm{r} = 0.5$ d is the sphere radius, ν is the fluid kinematical viscosity, $\bar{V}$ is the vector of the translational sphere velocity, and $\bar{\omega}$ is the vector of angular velocity of the sphere rotation about its centre of mass, which coincides with its geometrical centre in the case of homogeneous sphere. Often the dimensionless parameter $\Gamma = r\,|\bar{\omega}|/|\bar{V}|$ is used instead of the rotational Reynolds number Re_ω (Oesterle and Dinh 1998). The parameter Γ is sometimes called dimensionless angular velocity. Any pair of these three dimensionless parameters, Re, Re_ω, and Γ, is equivalent to the others and $\Gamma = 2\ \mathrm{Re}_\omega/\mathrm{Re}$.

The present research is focused mainly on evaluation of the drag force, drag torque, and Magnus force acting on a rotating sphere moving in viscous fluid. The drag force acting on a sphere moving in fluid translationally without rotation is well known (Niño and García 1994). Sufficient information is also known about the drag torque acting on the sphere rotating in fluid without translational motion (Sawatzki 1970). However, experimental and theoretical data on the drag force and the drag torque in the case when the sphere moves translationally and rotates simultaneously are described in the literature insufficiently for use in numerical models. It will be shown that in this case the mutual influences of the translational and rotational particle movements should be taken into account.

Similarly, there is also a shortage of detailed information about the Magnus force and its dependency on both translational and rotational sphere motion. The basic relationships for these forces and torque can be expressed from dimensional analysis and the dimensionless coefficients should be determined experimentally in dependence on both translational and rotational Reynolds numbers.

Drag Force, Drag Torque, and Magnus Force

The value of the drag force per unit volume acting on a sphere moving in fluid can be described by the following formula:

$$\bar{F}_d = -\frac{3}{4}\rho\frac{C_d}{d}\,|\,\bar{V}|\,\bar{V}, \tag{1}$$

where ρ is the fluid density and $\mathrm{C_d}$ is the dimensionless drag force coefficient. In the case of the sphere translational motion without rotation ($\mathrm{Re}_\omega = 0$), the drag force coefficient $\mathrm{C_d} = \mathrm{C_d}\ (\mathrm{Re},\ \mathrm{Re}_\omega = 0) = \mathrm{C_{d0}}\ (\mathrm{Re})$ is described well by the following expression (Niño and García 1994):

$$C_{d0} = \frac{24}{\mathrm{Re}}\left(1 + 0.15\,\mathrm{Re}^{\frac{1}{2}} + 0.017\,\mathrm{Re}\right) - \frac{0.208}{1 + 10^4\mathrm{Re}^{-0.5}}. \tag{2}$$

This expression is valid in a wide range of values of the Reynolds number, and for small Reynolds numbers ($\mathrm{Re} \to 0$) is transformed to the well-known Stokes drag.

The drag torque acting on a sphere rotating around its diameter in fluid depends on values of its angular velocity and size as well as the density and viscosity of fluid. Its value is given by the formula:

$$\bar{M} = -C_\omega \frac{\rho}{2} \bar{\omega} \,|\, \bar{\omega} \,| \, r^5, \tag{3}$$

where C_ω is the dimensionless drag torque coefficient. The reliable experimental and theoretical data of the dimensionless dependence $C_\omega = C_\omega\,(\mathrm{Re} = 0, \mathrm{Re}_\omega) = C_{\omega 0}\,(\mathrm{Re}_\omega)$ are described by Sawatzki (1970) for a sphere rotating with constant angular velocity in viscous fluid, which is at rest at a large distance from the rotating sphere.

The lateral Magnus force per unit volume is defined by Rubinov and Keller (1961) and Nigmatulin (1987):

$$\bar{F}_M = C_M \rho [\bar{\omega} \times \bar{V}], \tag{4}$$

where C_M is the dimensionless Magnus force coefficient.

Sometimes the dimensionless coefficient of the Magnus force is introduced differently. Barkla and Auchterlonie (1971), Tsuji et al. (1985), Oesterle and Dinh (1998), used the following expression for the lift coefficient C_L:

$$C_L = \frac{F_L}{0.5 * \rho |\bar{V}|^2 A}, \tag{5}$$

where $A = 0.25\pi d^2$ is the frontal (or the projected sectional) area of the sphere and

$$F_L = \frac{1}{6} \pi d^3 F_M. \tag{6}$$

The correlation between the lift coefficient C_L and Magnus force coefficient C_M is

$$C_L = \frac{8\Gamma}{3} C_M. \tag{7}$$

Equation (4) seems more preferable than Equation (5) because Equation (4) reflects directly the dependence of the Magnus force not only on the translational velocity but also on the angular velocity.

The phenomenon of the lateral force formation in the case of translational and simultaneously rotational sphere motion in fluid is commonly known as the Magnus effect. However, the successful experiments were carried out by Magnus (1853) with rotating cylinders, and were purely qualitative. The same effect of rotating spheres was known nearly two centuries sooner. Many researchers, including Newton, Poisson, Euler, Rayleigh and Tait, have investigated this problem (Maccoll 1928). The usual explanation of the phenomenon is that rotating sphere produces a swirl of fluid around it and the swirl modifies the uniform flow of fluid. As a result, the pressure is diminished on one side of the sphere and increased on the other side that gives a side thrust.

The first experimental study, seemingly, was carried out by Maccol (1928). He used the wood spheres, rotating in air stream, and obtained the dependences of

the drag force and Magnus force coefficients on the dimensionless angular velocity Γ for a few values of the Reynolds number Re. He revealed that the Magnus force coefficient is negative for $0 < \Gamma < 0.5$ and increases steeply in the range $0.5 < \Gamma < 1.5$. He also explored the flow on the rear of a rotating sphere and established the existence of vortices behind the sphere.

Davies (1949) studied the aerodynamic force acting on the golf balls in air stream. He obtained the dependence of the Magnus force on the angular velocity and showed that surface roughness increases this force.

The theoretical analysis of the Magnus force was performed by Rubinov and Keller (1961) for $\mathrm{Re} \ll 1$ and $\mathrm{Re}_\omega \ll 1$. They deduced $C_M = 3/4$. Goldshtik and Sorokin (1968) gave the theoretical evaluation $C_M = 2$ for the values of Reynolds numbers $\mathrm{Re} \gg 1$ and $\mathrm{Re}_\omega \gg 1$.

Using a conical pendulum technique, Barkla and Auchterlonie (1971) estimated the drag force coefficient and lift force coefficient of a sphere rotating in the air in the range of moderate Reynolds numbers $1{,}500 < \mathrm{Re} < 3{,}000$ and $0 < \Gamma < 12$.

In the range of moderate Reynolds numbers Tsuji et al. (1985) observed trajectories of the sphere, which collided with an inclined plate submerged in water and bounced. The trajectories were compared with the numerically calculated ones. The experiments were conducted for the Reynolds number range $550 < \mathrm{Re} < 1{,}600$ and the dimensionless angular velocity $\Gamma < 0.7$, and the coefficient C_M was evaluated as: $C_M = 0.15 \pm 0.04$.

Tanaka et al. (1990) measured the Magnus (lift) and drag forces of rotating sphere and spheroid. The Reynolds number of the measured bodies ranges from 60,000 to 150,000. In the case of the sphere, the negative lift force coefficient was observed at the Reynolds number higher than 100,000 and the dimensionless angular velocity $0.3 < \Gamma < 0.55$.

Oesterle and Dinh (1998) proposed the following experimental correlation for the Reynolds number range $10 < \mathrm{Re} < 140$ and the dimensionless angular velocity $1 < \Gamma < 6$:

$$C_L \approx 0.45 + (2\Gamma - 0.45)\exp\left(-0.075\Gamma^{0.4}\mathrm{Re}^{0.7}\right) \tag{8}$$

Lukerchenko et al. (2008) studied the mutual influence of the translational and rotational motion of a spherical ball in fluid using experiments and numerical simulation for the Reynolds numbers range $2{,}000 \le \mathrm{Re} \le 20{,}000$ and $2{,}000 \le \mathrm{Re}_\omega \le 20{,}000$. The formulas for the drag force and drag torque coefficients as functions of both Reynolds numbers were developed.

In contradiction to the previous one, the present paper also deals with the Magnus force coefficient. The experiments were conducted in a bigger vessel, which decreased the effect of the vessel walls, and a special spinning device was used which made it possible to reach higher values of the angular particle velocity ω and dimensionless angular particle velocity Γ. The results of the previous and present works are summarized and the common conclusions are presented.

The dependences $C_{d0}(\mathrm{Re})$ and $C_{\omega 0}(\mathrm{Re}_\omega)$ are valid for a steady motion of the sphere. They can be also used for quasi-steady motion of the sphere, that is, if the sphere moves with relatively small accelerations. Similarly, for a free quasi-steady motion of a sphere in fluid (without any other disturbances) we can consider that C_d, C_ω, and C_M depend only on Re and Re_ω.

Mathematical Model of the Motion of a Sphere in Fluid

The system of equations describing the motion of a sphere in fluid is (Lukerchenko et al. 2006):

$$\rho_p \frac{d\bar{V}}{dt} = \bar{F}_d + \bar{F}_g + \bar{F}_M + \bar{F}_m, \tag{9}$$

$$J \frac{d\bar{\omega}}{dt} = \bar{M}, \tag{10}$$

where ρ_p is the sphere density and J is the sphere momentum of inertia. The individual terms of the right-hand side of Equation (9) are the following forces per unit volume: drag force $\bar{F}_D$, Magnus force $\bar{F}_M$, submerged gravitational force

$$\bar{F}_g = \left(\rho_p - \rho\right) \bar{g}, \tag{11}$$

and the added mass force

$$\bar{F}_m = -\rho\, C_m \frac{d\bar{V}}{dt}, \tag{12}$$

where $\bar{g}$ is the vector of the gravitational acceleration and $C_m = 0.5$ is the added mass coefficient.

In addition to the above mentioned forces, the two-dimensional numerical model of the motion of a sphere (Lukerchenko et al. 2006) includes the Basset history force, which mathematically represents the product of a constant factor by the integral, of which the integrand comprises the sphere acceleration as the multiplier. However, it is shown (e.g., Bombardelli et al. 2008; Lukerchenko 2010a, 2010b) that the Basset history force is important only for relatively small spherical particles, whereas relatively large spherical particles were used (d = 0.0146–0.0365 m) in the present study. Moreover, as was mentioned above and will be discussed later, we consider only the part of the ball trajectory in which the particle motion is quasi-steady, that is, the ball acceleration is relatively small. For that reason the initial unsteady part of the particle trajectory in water is disregarded. In the other part of the trajectory the particle acceleration is negligible and therefore the values of the integrand and integral become small and the Basset history force can be practically neglected. The test calculation showed that the Basset history force was small in the quasi-steady part of the particle trajectory, and therefore in the subsequent simulations this force was not taken into account.

Let us consider only the case $\bar{\omega} \perp \bar{V}$. If $\bar{\omega} \perp \bar{g}$ also (the vector $\bar{V}$ is in a vertical plane); then the trajectory of sphere center is two-dimensional and lies on a vertical plane. The change in the modulus of the translational velocity $\bar{V}$ allows us to evaluate the drag force, that is, the drag force coefficient C_d. The change in the modulus of the angular velocity $\bar{\omega}$ allows us to evaluate the drag torque, that is, the drag torque coefficient C_ω. The trajectory curvature allows us to evaluate the Magnus force, that is, the Magnus force coefficient C_M.

Experimental Procedure

Two series of the experiments, C and D, were realized. The experimental series C were carried out in a rectangular glass vessel 0.283 m long, 0.184 m wide, and 0.790 m high. The water depth varied from 0.710 to 0.740 m. Each measured spherical particle of series C was speeded up in the special chute (see Figure 1a), which ensured the required angular and translational velocities of the particle in the given plane (coordinate plane Oxy; the axis x is horizontal and the axis y is vertical). Different levels of the initial height of the particle in the chute were used to provide different values of the initial translational and angular velocities of the individual particle. In this case the initial translational and angular particle velocities are mutually dependent: $|\bar{V}| = |\bar{\omega}|r\sin(\alpha/2)$ or $\Gamma = \sin^{-1}(\alpha/2)$, where α is the opening angle of the chute ($0 < \alpha < \pi$). The chute with the opening angle $\alpha = \pi/2$ was used (i.e., $\Gamma = 2^{0.5}$).

The experimental series D were carried out in a bigger rectangular glass vessel 0.780 m long, 0.580 m wide, and 0.980 m high. The water depth was 0.800 m. Each measured particle of series D was speeded up in a special device (developed in the Institute of Hydrodynamics AS CR, v. v. i.) situated above the water level (see Figure 1b). The particle was held between cups and rotated about a horizontal axis with a variable angular velocity. When the trigger was released, the springs pulled the cups apart, allowing the particle to fall freely in water. The spinning device ensured the required particle rotation in the given plane, and translational velocity of the particle was reached by free fall. The device allows the particle to be spun up to 5000

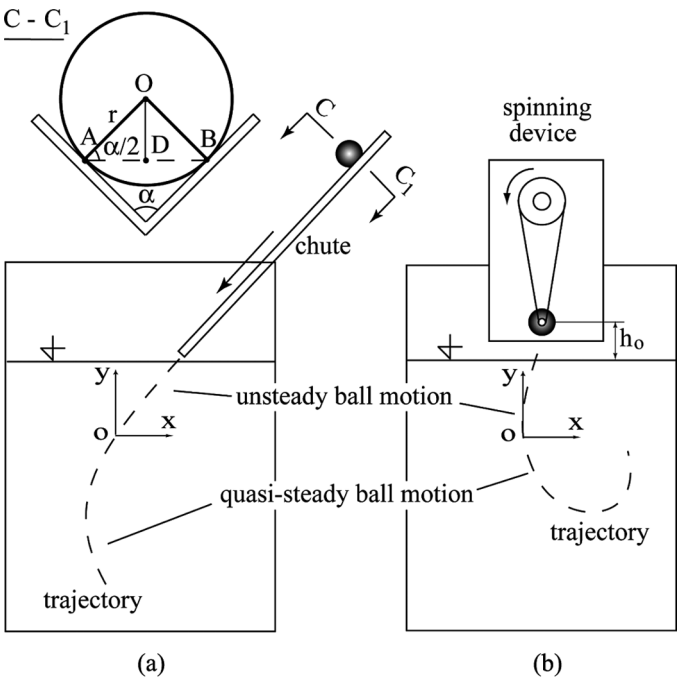

Figure 1. Schematic view of the experimental setup: a) experimental series C; AB – instantaneous axis of the ball rotation; OD = r sin(α/2) – instantaneous radius of the ball rotation b) experimental series D.

revolutions per minute. The translational velocity of the particle was given by the height h_0 of the device above the water surface. The initial translational and angular particle velocities can be chosen independently from one other.

Two model spherical particles, ball A ($\rho_p = 1030\,kg/m^3$, $m = 0.0257\,kg$, $d = 0.0363\,m$) and ball B ($\rho_p = 971\,kg/m^3$, $m = 0.0247\,kg$; $d = 0.0365\,m$) were used in experimental series D.

As they follow from the dimensional analysis the drag force, drag torque and Magnus force coefficients are independent of the particle density and hence can be chosen arbitrarily. For this reason in both series the rubber spherical balls with densities near to that of water were chosen, making it possible to use the video system recording images at rates of 25 and 50 frames per second for the visualization. From 150 to 200 images were made for each experiment. Hairlines were drawn on the balls along two perimeters of the balls with the angle of 90° to make it possible to visualize the ball rotation. Only experiments in which the plane of the particle trajectory was parallel to the plane of the video camera objective were evaluated. The geometric and kinematical properties of the ball motion were found from the image sequences.

Results

The system of Equations (9) and (10) describing the spherical particle motion in fluid was solved numerically. The experimental and calculated trajectories and the ball kinematical parameters were plotted as functions of time. The values of the drag torque coefficient C_ω, drag force coefficient C_d, and Magnus force coefficient C_M were found using the method of best fit of the experimental data.

First, the method of definition of the drag force coefficient from comparison of the results of simulation with the experimental data was tested. The experiments with the ball angular velocity equal to zero were evaluated. The typical plot of the ball velocity versus time for experimental and simulated translational ball velocity is shown in Figure 2. The value of time $t = 0$ corresponds to the moment of the ball's entry in water.

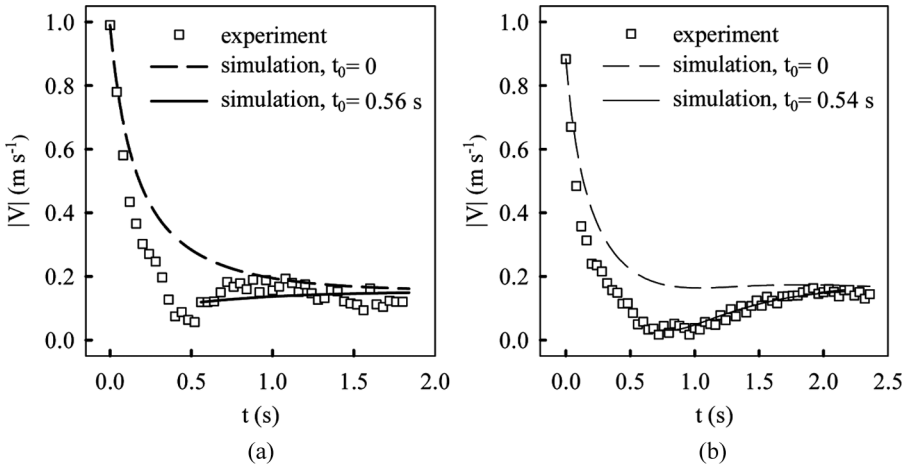

Figure 2. Comparison of the experimental and calculated ball translational velocities $\bar{V}$ ($h_0 = 0.10\,m$, $Re_\omega = 0$): *a*) ball A; b) ball B.

The initial part of the ball trajectory immediately after its entry in water was neglected because the ball motion is unsteady in this part, whereas we assumed that the ball motion is quasi-steady. The additional forces act on the ball in the initial part of its movement in water due to the different disturbances (transition of the ball from air to water, effect of air bubbles on the ball surface, etc.).

The numerical model used does not take into account these disturbances and therefore it cannot give results, which agreed satisfactorily with the experimental data for the initial part of the ball motion. If the calculations are carried out from the moment of the ball's entry in water $t_0 = 0$, the calculated ball velocity differs sharply from the experimental one in the initial part of the ball trajectory (see Figure 2). When the simulation starts in the moment t_0, that is, the calculation of the ball motion is carried out from time $t = t_0$, the discrepancy becomes smaller. The calculated and experimental data agree satisfactorily when the simulation starts in the moment $t_0 = 0.56$ s for ball A, and $t_0 = 0.54$ s for ball B, that is, in the moment when quasi-steady motion begins and disturbances due to the particle's entry into the water become negligible. Figure 2 illustrates the case of the height of the spinning device above the water surface $h_0 = 0.1$ m. If the value of h_0 decreases, the length of the initial unsteady part of the ball trajectory also decreases.

Part of the experimental results of series C was presented in Lukerchenko et al. (2008). It is shown for the Reynolds numbers $\mathrm{Re} < 20{,}000$ and $\mathrm{Re}_\omega < 20{,}000$ (the value of the dimensionless angular velocity Γ during each experiment was changed but it was less than 3.5) that the coefficients of the drag force C_d and drag torque C_ω depend on both translational and rotational Reynolds numbers and can be expressed by the simple formulas:

$$C_d = C_{d0}\left(1 + 0.065\ Re_{\omega}^{0.3}\right), \tag{13}$$

$$C_\omega = C_{\omega 0}\left(1 + 0.0044\, Re^{0.5}\right). \tag{14}$$

It was determined in the experimental series C that the Magnus force coefficient lies in the range $0.023 < C_M < 0.048$. These values are significantly less than the theoretically predicted value, which is equal to 0.75 (Rubinov and Keller 1961) or 2 (Goldshtik and Sorokin 1968).

According to Equation (13), $C_d > C_{d0}$. However, Barkla and Auchterlonie (1971) showed that the values of C_d are lower than C_{d0} when the parameter $\Gamma > 5$. The device used in the experimental series D allowed the ball to be spun up so that the dimensionless angular velocity Γ varied in the range from 0 to 12.

The experimental series D were carried out for a relatively slow ball rotation ($\Gamma < 3.5$) and also for the relatively fast ball rotation ($5 < \Gamma < 10$). The values of the Reynolds numbers in both cases were in the ranges $5{,}000 < \mathrm{Re} < 20{,}000$ and $3{,}000 < \mathrm{Re}_\omega < 20{,}000$. Further, comparison of calculated and experimental results of ball angular velocity, dimensionless ball angular velocity, and transitional ball velocity obtained for two balls, ball A with a density larger than that of water ($\rho_p = 1030\ \mathrm{kg/m^3}$) and ball B with a density less than that of water ($\rho_p = 971\ \mathrm{kg/m^3}$), are presented in Figures 3–5. The moment $t = 0$ corresponds to the beginning of the quasi-steady part of the ball motion t_0. The relatively slow ball rotation ($1.6 < \Gamma < 3.5$) was realized with ball A (initial ball angular velocity $\omega_0 = 60\ \mathrm{s^{-1}}$), the relatively fast rotation was realized with ball B ($5 < \Gamma < 10$ on the substantial part

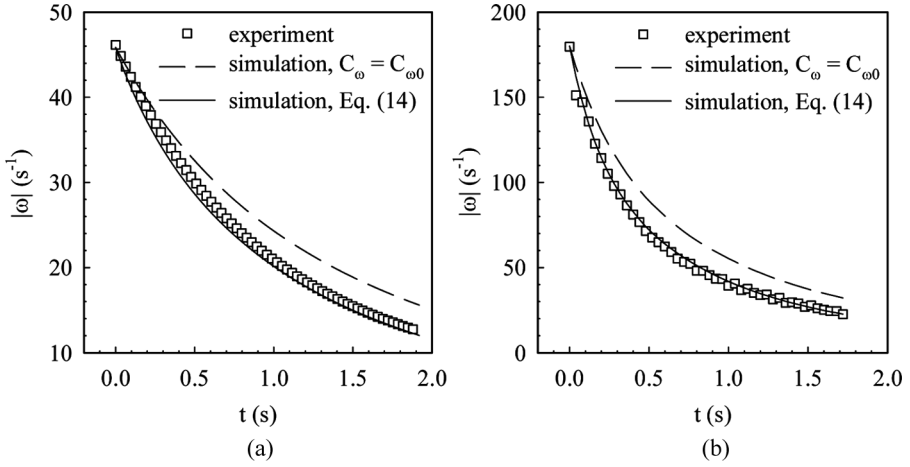

Figure 3. Ball angular velocity $\bar{\omega}$ versus time t: a) ball A, slow rotation, b) ball B, fast rotation.

of the trajectory and $\omega_0 = 300\,\mathrm{s}^{-1}$); height of the spinning device above the water level $h_0 = 0.02\,\mathrm{m}$.

The dependences of the ball angular velocity versus time are shown in Figure 3. In both cases the values of the ball angular velocity calculated without taking into account the translational ball motion (i.e., for $\mathrm{Re} = 0$) are larger than the experimental values. The values of angular velocity calculated with the help of Equation (14) show good agreement with experimental ones. The corresponding values of the dimensionless angular velocity Γ are shown in Figure 4 (the experimental data were smoothed by the polynomial function).

Good agreements between the calculated and experimental values of translational ball velocity are obtained in the case of slow particle rotation (see Figure 5a) if the coefficient C_d is calculated using the Equation (13) and in the case of relatively

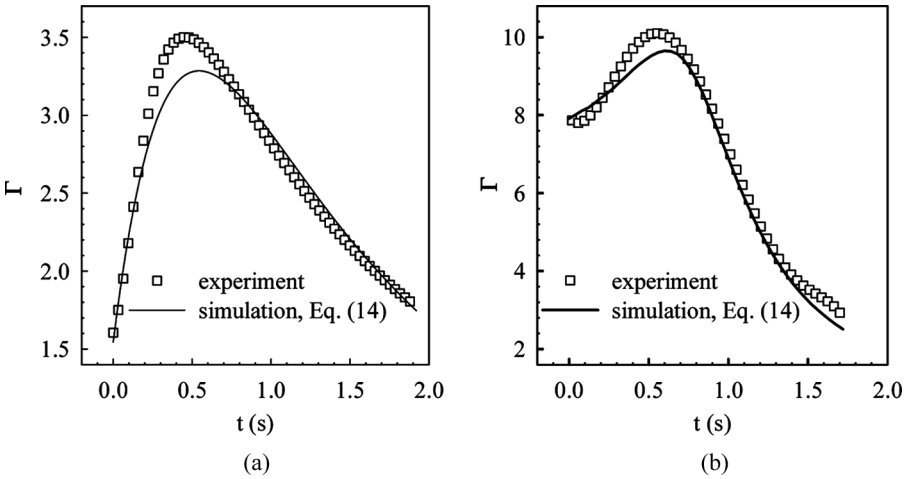

Figure 4. Dimensionless angular velocity Γ versus time t: a) ball A, slow rotation, b) ball B, fast rotation.

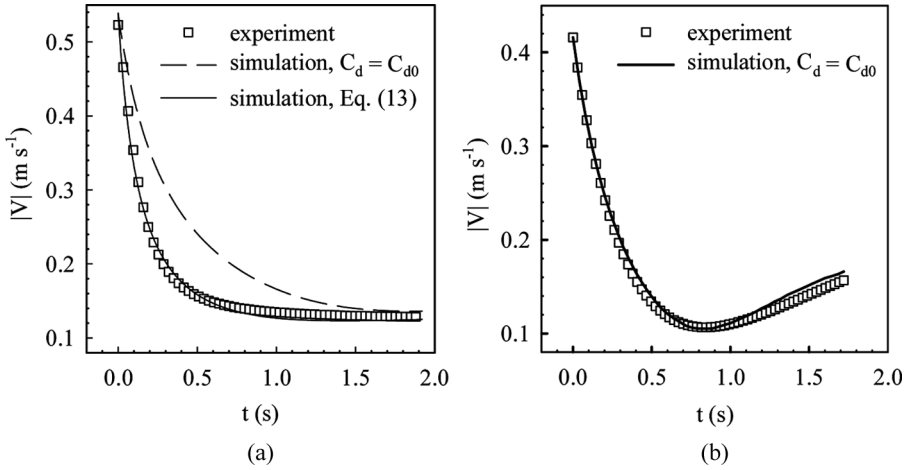

Figure 5. Transitional ball center velocity $\bar{V}$ versus time t: a) ball A, slow rotation, b) ball B, fast rotation.

fast particle rotation (see Figure 5b) if the relationship $C_d = C_{d0}$ is used (the experimental data were smoothed by the exponential decay function).

The trajectories of the ball's centre are presented in Figure 6. The origins of the coordinate system are chosen at the beginning of the quasi-steady part of the ball trajectory. Good agreements between the calculated and experimental ball trajectories are reached in the case of calculations of the Magnus force coefficient $C_M = 0.04$ for relatively slow particle rotation (see Figure 6a) and when the Magnus force coefficient for relatively fast particle rotation is calculated according to the following simple formula (see Figure 6b):

$$C_M = 0.07/\Gamma \tag{15}$$

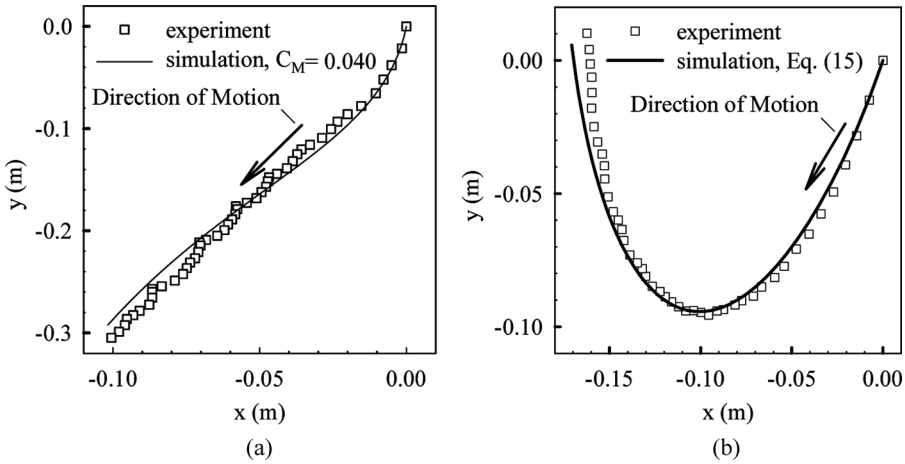

Figure 6. Transitional ball centre trajectory: a) ball A, slow rotation, b) ball B, fast rotation.

Thus, for the fast rotating spherical particle ($5 < \Gamma < 12$) the value of the drag force coefficient C_d can be taken as equal to C_{d0} and the value of the Magnus force coefficient C_M can be calculated according to Equation (15).

Conclusions

The mutual influence of the translational and rotational spherical particle movements in fluid was studied using the experimental data and the numerical simulation. The drag force coefficient, drag moment coefficient, and Magnus force coefficient of a spherical particle were evaluated for the case of simultaneous translational and rotational particle motion in calm water for the Reynolds numbers ranges $5{,}000 < \mathrm{Re} < 20{,}000$ and $3{,}000 < \mathrm{Re}_\omega < 20{,}000$.

Two cases were studied: firstly, relatively slow rotation ($\Gamma < 3.5$) and, secondly, relatively fast rotation ($5 < \Gamma < 12$). The following results can be emphasized:

- For the drag torque coefficient C_ω Equation (14) is valid in both cases.
- For the drag force coefficient C_d Equation (13) is valid if $1 < \Gamma < 3.5$ and $C_d = C_{d0}$ if $5 < \Gamma < 12$.
- The value of the Magnus force coefficient C_M varies from 0.023 to 0.048 if the dimensionless angular velocity $\Gamma < 3.5$ and Equation (15) can be used if $5 < \Gamma < 12$.

The results are useful for numerical simulation of the particle motion in fluid and modeling of the particle-laden flow and sediment transport of sand in rivers.

List of Symbols

A	frontal (or the projected sectional) area of the sphere, m^2
C_d	drag force coefficient
C_{d0}	drag force coefficient for the particle moving in fluid without rotation
C_L	lift coefficient
C_m	added mass coefficient
C_M	Magnus force coefficient
C_ω	drag rotation coefficient
$C_{\omega 0}$	drag rotation coefficient for the particle rotating in fluid without a displacement
d	particle diameter, m
$\bar{F}_D$	drag force per unit volume, $\mathrm{N\,m^{-3}}$
$\bar{F}_g$	submerged gravitational force per unit volume, $\mathrm{N\,m^{-3}}$
$\bar{F}_L$	lift force, N
$\bar{F}_m$	added mass force per unit volume, $\mathrm{N\,m^{-3}}$
$\bar{F}_M$	Magnus force per unit volume, $\mathrm{N\,m^{-3}}$
$\bar{g}$	gravitational acceleration, $\mathrm{ms^{-2}}$
h_0	height of the device above the water surface, m
J	particle momentum of inertia, $\mathrm{kg\,m^2}$
m	particle mass, kg
$\bar{M}$	torque of the force acting on the rotating particle in fluid, N m
r	particle radius, m
Re	particle (translational) Reynolds number
Re_ω	particle rotational Reynolds number

t	time, s
t_0	starting time of the simulation, s
$\bar{V}$	vector of the particle translational velocity, ms^{-1}
α	opening angle of the chute
Γ	dimensionless particle angular velocity
ν	kinematical fluid viscosity, $m^2 s^{-1}$
ρ	fluid density, $kg\,m^{-3}$
ρ_p	particle density, $kg\,m^{-3}$
$\bar{\omega}$	vector of the particle angular velocity, s^{-1}

References

Barkla, H. M., and L. J. Auchterlonie. 1971. The Magnus or Robins effect on rotating spheres. *Journal of Fluid Mechanics* 47 (3): 437–447.

Bombardelli, F. A., A. E. González, and Y. I. Niño. 2008. Computation of the particle Basset force with a fractional-derivative approach. *Journal of Hydraulics Engineering* 134 (10): 1513–1520.

Chara, Z., I. Ivanova, N. Lukerchenko, and P. Vlasak. 2009. Influence of Inflow Conditions on Saltation Movement of Spherical Particles. In *Proceedings of Int. Conf. Numerical Analysis and Applied Mathematics, Rethymno, Crete, Greece, 18–22 September 2009*, eds. Th. E. Simos, G. Psihoyios, and Ch. Tsitouras, pp. 613–616. Melville, NY: American Institute of Physics.

Davies, J. M. 1949. The aerodynamics of golf balls. *Journal Applied Physics* 20: 821–828.

Goldshtik, M. A., and V. N. Sorokin. 1968. On motion of particle in vortex chamber. *Journal of Applied Mathematics and Technical Physics* 6: 149–152. (in Russian)

Kholpanov, L. P., and R. I. Ibyatov. 2005. Mathematical modelling of the dispersed phase dynamics. *Theoretical Foundations of Chemical Engineering* 39 (2): 190–199.

Lukerchenko, N. 2010a. Discussion of "Computation of the Particle Basset Force with a Fractional-Derivative Approach" by Fabián A. Bombardelli, Andrea E. González, and Yarko I. Niño. *Journal of Hydraulic Engineering ASME* 136 (10): 853–854.

Lukerchenko, N. 2010b. Basset history force for the bed load sediment transport. In *Proceedings of the First IAHR European Division Congress, 4–6 May 2010*, Edinburgh, Scotland, Heriot-Watt University. Book of Abstracts: 7 (CD ROM-Pap. FMIId).

Lukerchenko, N., Z. Chara, and P. Vlasak. 2006. 2D numerical model of particle-bed collision in fluid-particle flows over bed. *Journal of Hydraulics Research* 44 (1): 70–78.

Lukerchenko, N., Yu. Kvurt, A. Kharlamov, Z. Chara, and P. Vlasak. 2008. Experimental evaluation of the drag force and drag torque acting on a rotating spherical particle moving in fluid. *Journal of Hydrology and Hydromechanics* 56 (2): 88–94.

Lukerchenko, N., S. Piatsevich, Z. Chara, Z., and P. Vlasak. 2009a. 3D numerical model of the spherical particle saltation in a channel with a rough fixed bed. *Journal of Hydrology and Hydromechanics* 57 (2): 100–112.

Lukerchenko, N., S. Piatsevich, Z. Chara, Z., and P. Vlasak. 2009b. Numerical model of the spherical particle saltation in channel with transversely tilted rough bed. *Journal of Hydrology and Hydromechanics* 57 (3): 182–190.

Maccol, J. W. 1928. Aerodynamics of a spinning sphere. *Journal of the Royal Aeronautical Society* 32: 777–798.

Magnus, G. 1853. Ueber die Abweichung der Geschosse, und eine auffallende Erscheinung bei rotirenden Körpern. *Poggendorfs Annalen der Physik und Chemie* 88: 1.

Oesterle, B., and T. Bui Dinh. 1998. Experiments on the lift of a spinning sphere in the range of intermediate Reynolds numbers. *Experimental Fluids* 25: 16–22.

Nigmatulin, R. I. 1987. *Dynamics of Multiphase Media.* Moscow: Nauka. Part I. (in Russian)

Niño, Y., and M. García. 1994. Gravel saltation. 2. Modeling. *Water Resources Research* 30 (6): 1915–1924.

Rubinov, S. I., and J. B. Keller. 1961. The transverse force on a spinning sphere moving in a viscous fluid. *Journal of Fluid Mechanics* 11: 447–459.

Sawatzki, O. 1970. Das Stromungsfeld um eine rotierende Kugel. *Acta Mechanica* 9: 159–214.

Tanaka, T., K. Yamagata, and Y. Tsuji. 1990. Experiment of fluid forces on a rotating sphere and spheroid. In *Proceedings of the SME-JSME Fluids Engineering Conference*, Seoul, Korea, vol. 1, pp. 366–369, October 10–13.

Tsuji, Y., Y. Morikawa, and O. Mizuno. 1985. Experimental measurements of the Magnus force on a rotating sphere at low Reynolds numbers. *ASME Journal of Fluid Engineering* 107: 484–488.